Nanoarchitectured $Na_6Fe_5(SO_4)_8$/CNTs cathode building a low-cost 3.6 V sodium-ion full battery with superior sodium storage

Shiyu Li [a, b,] , Xiaosheng Song [c], Xiaoxiao Kuai [a, b], Wenchang Zhu [a, b], Kai Tian [a, b], Xifei Li [c,*], Mingzhe Chen [d], Shulei Chou [d], Jianqing Zhao [a, b, *], Lijun Gao [a, b, *]

[a.] *College of Energy, Soochow Institute for Energy and Materials InnovationS, Soochow University, Suzhou 215006, P. R. China.*
[b.] *Key Laboratory of Advanced Carbon Materials and Wearable Energy Technologies of Jiangsu Province, Soochow University, Suzhou 215006, P. R. China.*
[c.] *Institute of Advanced Electrochemical Energy & School of Materials Science and Engineering, Xi'an University of Technology, Xi'an, Shaanxi 710048, P. R. China.*
[d.] *Institute for Superconducting and Electronic Materials, Australian Institute for Innovative Materials, University of Wollongong, North Wollongong NSW 2522, Australia.*
**Corresponding author E-mail: gaolijun@suda.edu.cn, jqzhao@suda.edu.cn, xfli2011@hotmail.com*

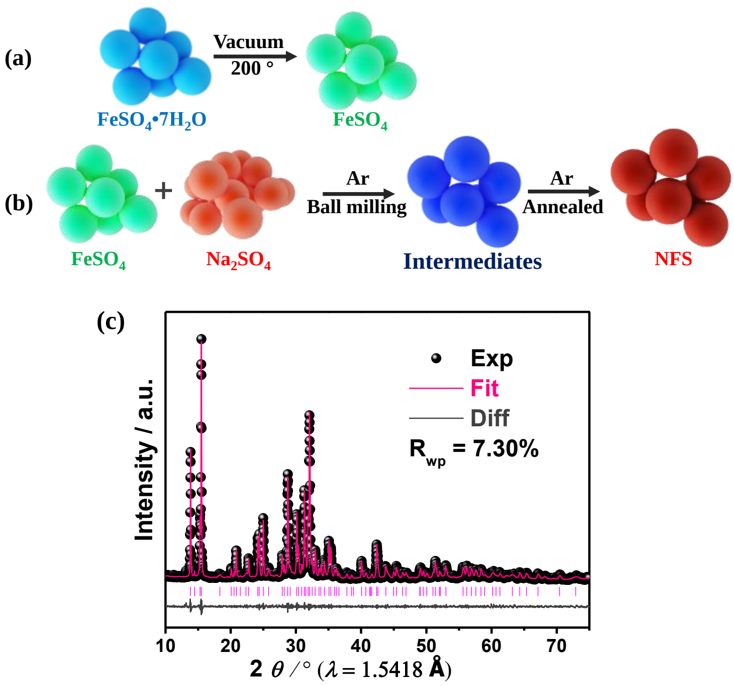

Figure S1. (a) Schematic illustration of synthetic processes for bare NFS material, and (b) XRD pattern of NFS material, coupled with Rietveld refinements (The black dots represent original experimental data, red line response calculated profile, pink lines display theoretical Bragg positions, and gray lines indicate differences between experimental and simulation results).

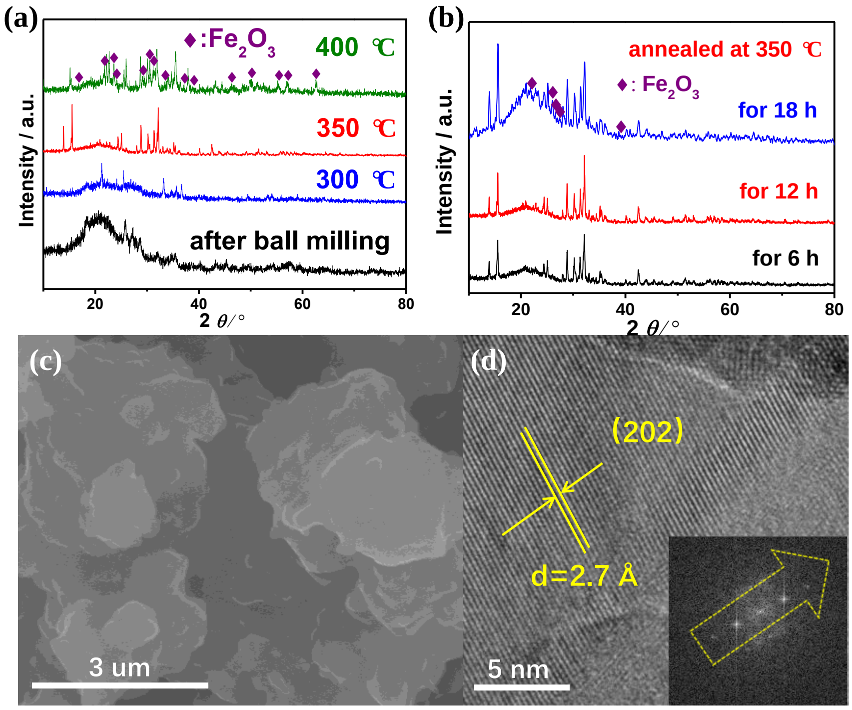

Figure S2. XRD patterns of the NFS@5%CNTs precursor annealed (a) at different temperatures after ball milling and (b) at 350 ℃ for different duration time, and (c) SEM image and (d) HRTEM image of bare NFS material.

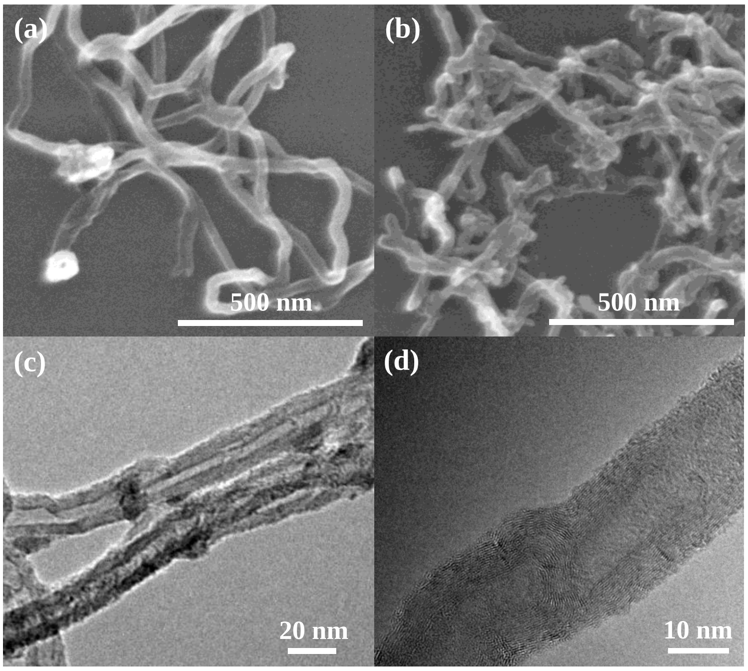

Figure S3. (a) SEM image, (c) TEM image, and (d) HRTEM image of CNTs material, (b) SEM image of residual CNTs material after treating NFS@5%CNTs in acidic HCl solution to dissolve the NFS component.

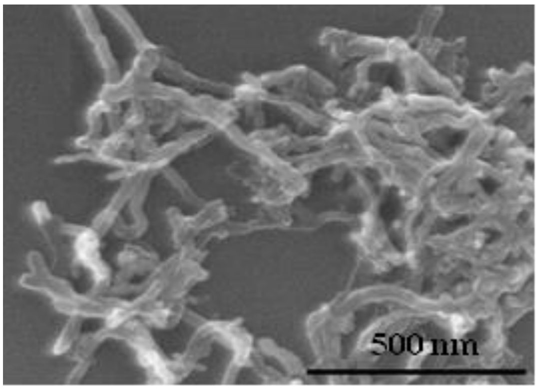

Figure S4. FESEM image of the residual CNTs after the NFS@5%CNTs powder was treated by the acid picking.

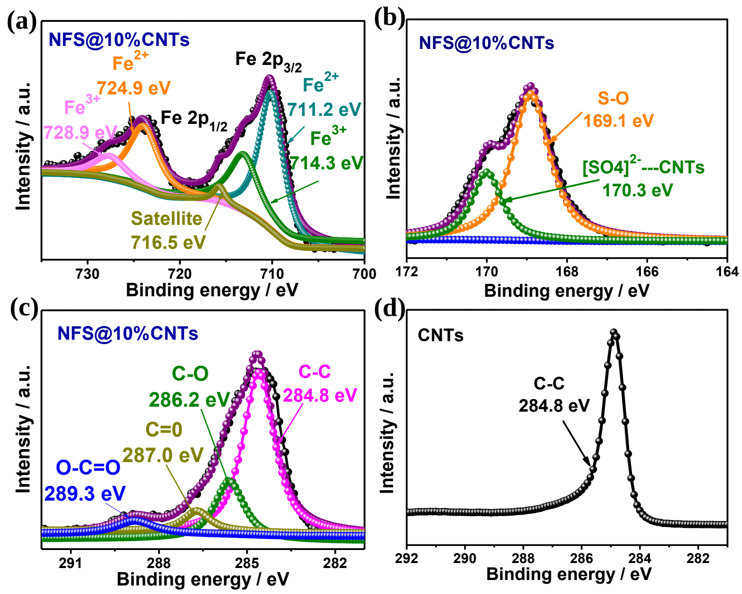

Figure S5. (a) Fe 2p, (b) S 2p and (c) C 1s XPS spectra of NFS@10%CNTs nanocomposite, and (d) characteristic C 1s XPS spectrum of CNTs material.

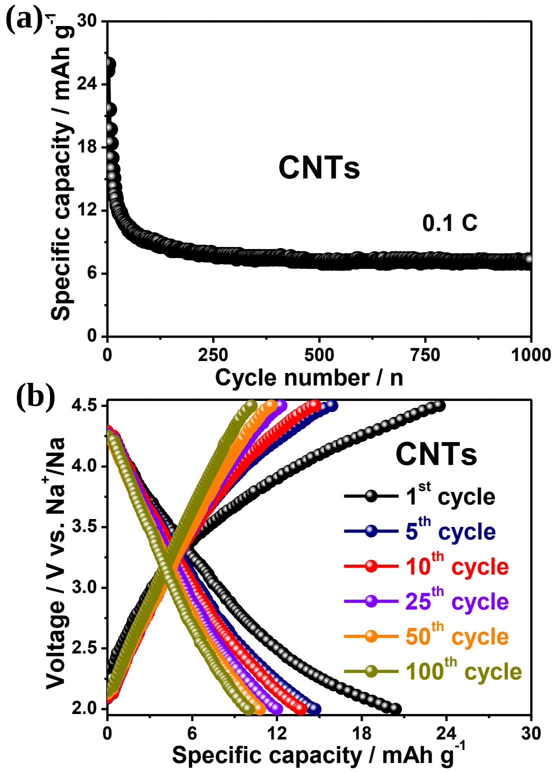

Figure S6. (a) Cycling performance and (b) corresponding charge/discharge curves in different cycles of CNTs material as the cathode for sodium-ion batteries at 0.1 *C* in a voltage range of 2.0-4.5 V *vs.* Na^+/Na.

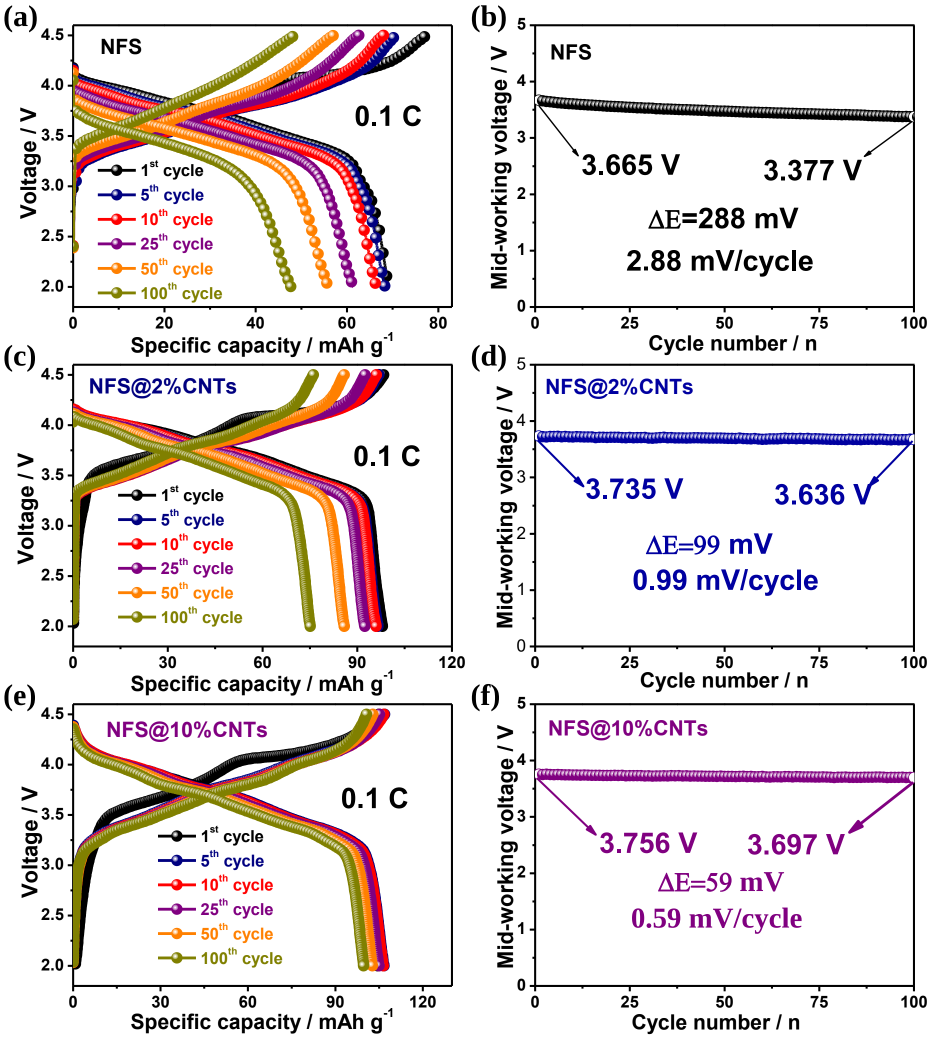

Figure S7. Charge/discharge curves and average working voltage per cycle of (a, b) bare NFS, (c, d) NFS@2%CNTs, and (e, f) NFS@10%CNTs cathode materials at 0.1 *C* in a voltage range of 2.0-4.5 V *vs.* Na^+/Na.

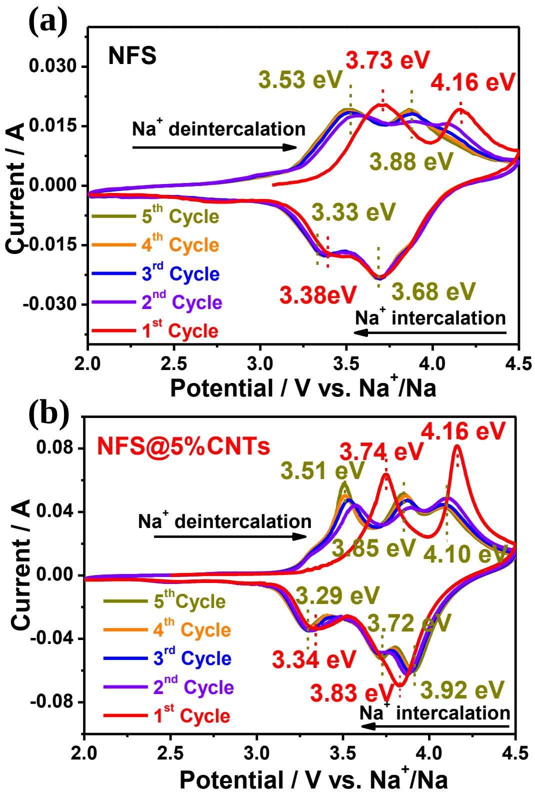

Figure S8. CV curves in the first five cycles of (a) bare NFS and (b) NFS@5%CNTs cathode materials recorded at a scanning rate of 0.1 mV s^{-1} in a voltage range of 2.0-4.5 V *vs.* Na^{+}/Na.

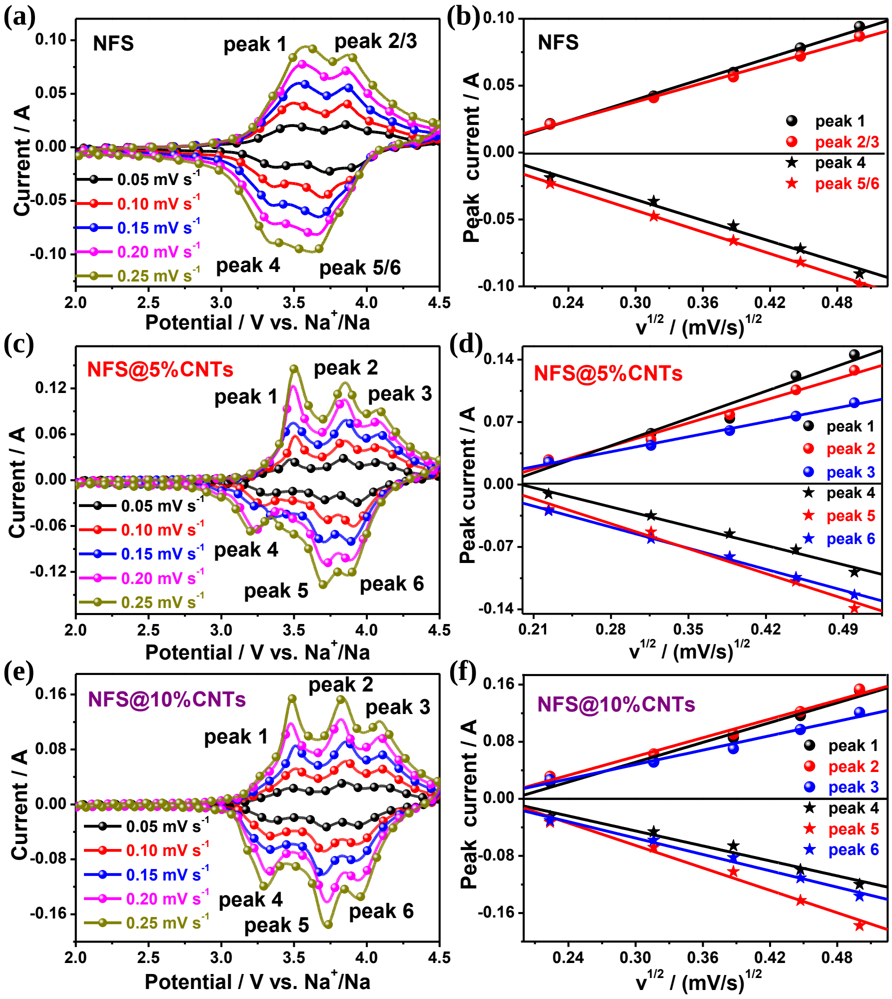

Figure S9. CV curves in the second cycle of (a) bare NFS, (c) NFS@5%CNTs, and (e) NFS@10%CNTs cathode materials recorded at different scanning rates of 0.05, 0.1, 0.15, 0.2, and 0.25 mV s^{-1}, and the relationship between anodic and cathodic peak currents (i_p) and the square root of scan rates ($v^{1/2}$) of (b) bare NFS, (d) NFS@5%CNTs, and (f) NFS@10%CNTs cathode materials.

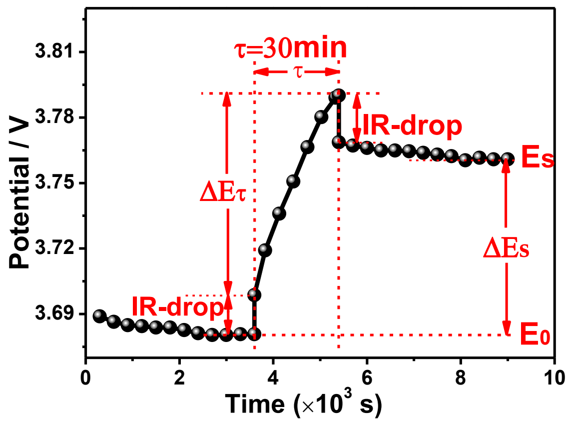

Figure S10. Enlarged voltage profiles for a single step of GITT curve at about 3.75 V during the charge of NFS@5%CNTs cathode material at 0.1 *C* as shown in Figure 5b.

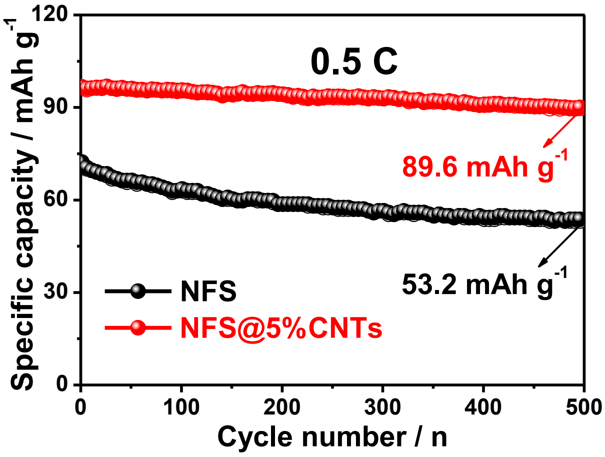

Figure S11. Cycling performance of bare NFS and NFS@5%CNTs cathode materials at 0.5 *C* in a voltage range of 2.0-4.5 V *vs.* Na^+/Na.

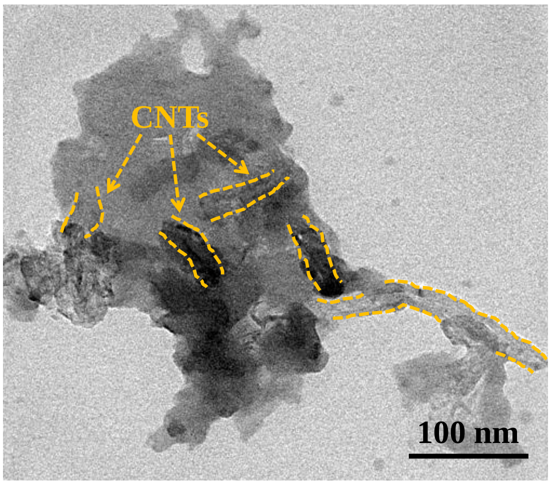

Figure S12. TEM image of the cycled NFS@5%CNTs cathode material.

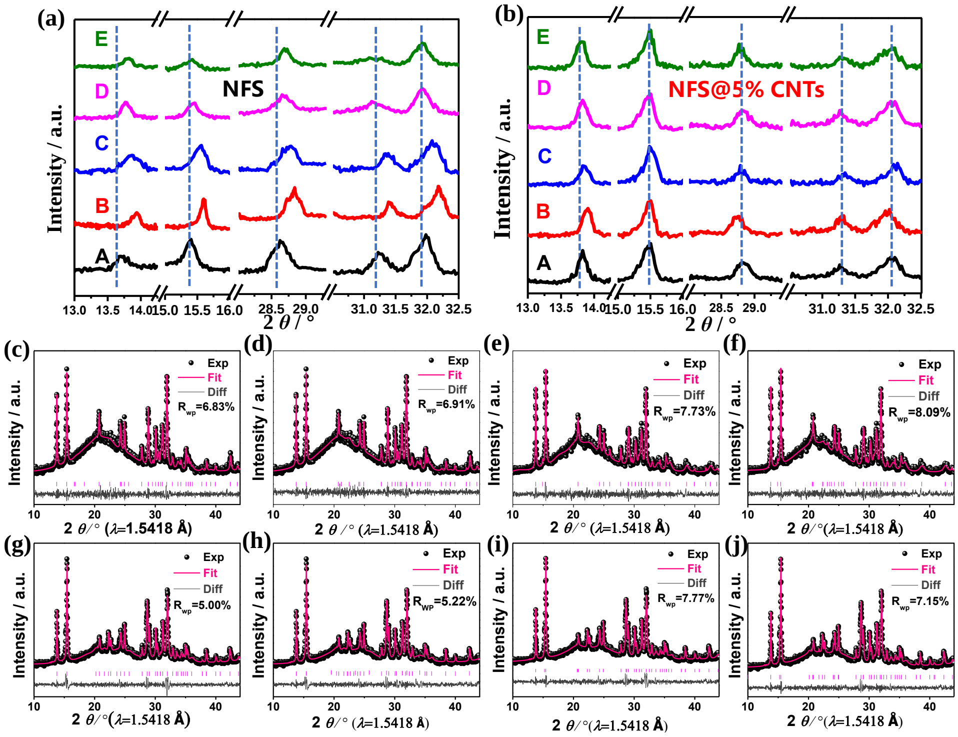

Figure S13. *Ex-situ* XRD patterns of cycled (a) bare NFS and (b) NFS@5%CNTs cathode materials at different working states (A: initial state before charge/discharge cycles, B: fully-charged to 4.5 V in the 1st cycle, C: fully-discharged to 2.0 V in the 1st cycle, D: fully-charged to 4.5 V in the 500th cycle, and E: fully-discharged to 2.0 V in the 500th cycle), and Rietveld refinement results of cycled (c-f) NFS and (g-j) NFS@5%CNTs cathode materials at B, C, D, and E states, respectively.

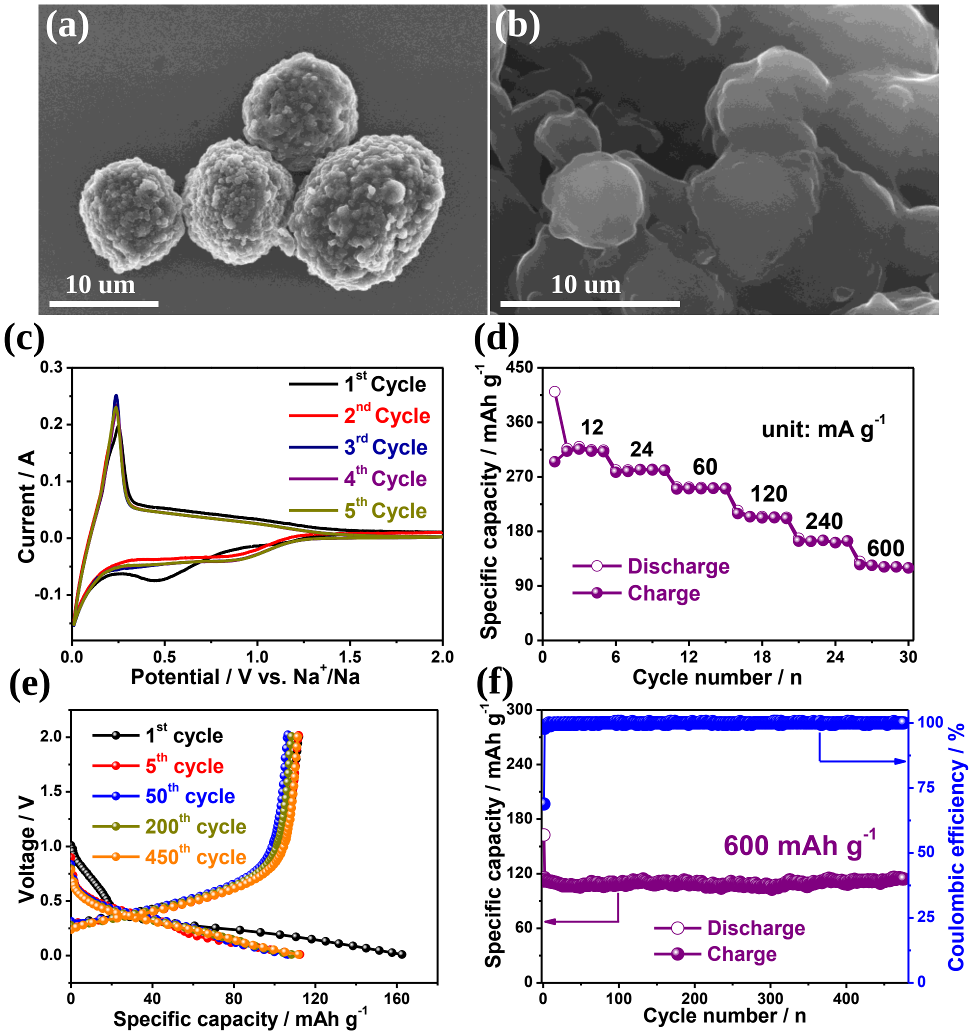

Figure S14. (a, b) SEM images, (c) CV cures in the first five cycles recorded at a scanning rate of 0.1 mV s^{-1}, (d) high-rate performance at different current densities, (e) discharge/charge curves in different cycles at 600 mA g^{-1} and (f) cycling performance at 600 mA g^{-1} of hard carbon as the anode material for sodium-ion batteries in a voltage range of 0.01-2.0 V *vs.* Na^+/Na.

Figure S15. The application of two cycled full NFS@5%CNTs//HC cells for lighteing a commercial LED study table lamp.

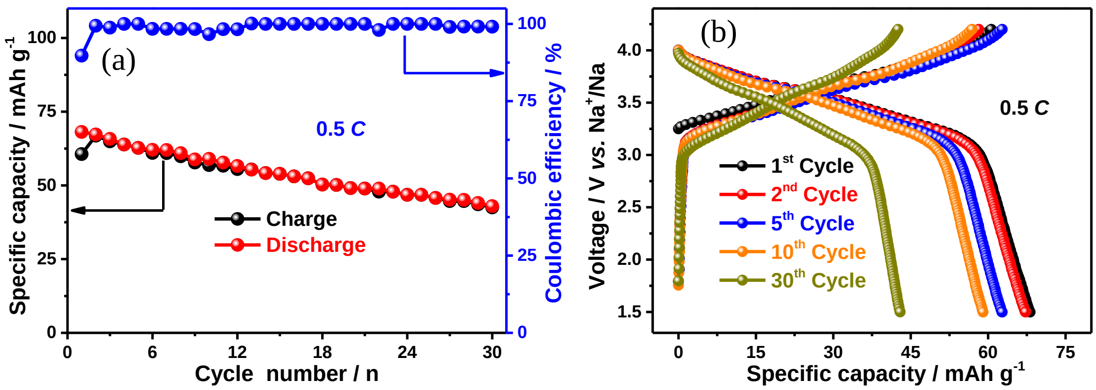

Figure S16. (a) Cycling performance of the NFS //HC full cell at 0.5 *C* and (b) corresponding charge/discharge curves in different cycles

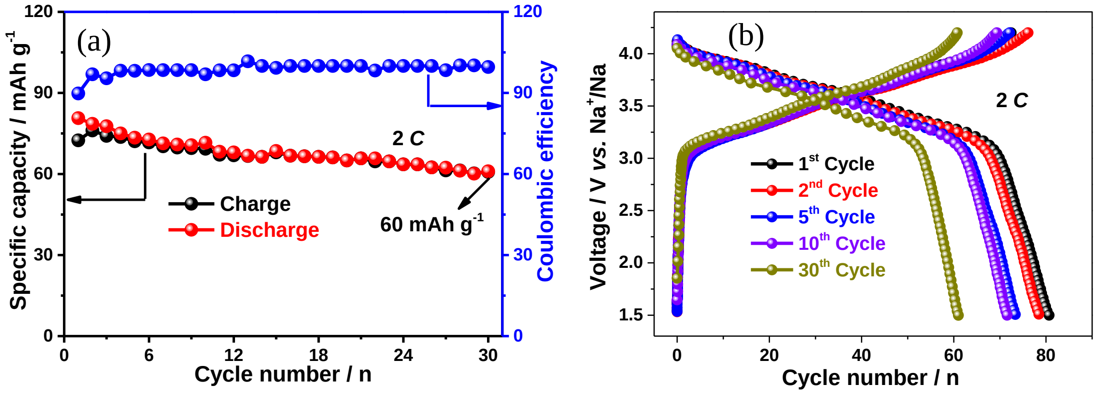

Figure S17. (a) Cycling performance of the NFS@5%CNTs//HC full cell at 2 *C* at 55 ℃ and (b) corresponding charge/discharge curves in different cycles.

Table S1. Lists of possible composite materials based on the solid solution of Na_2SO_4 and $FeSO_4$ components at different molar ratios.

	Na^+=a a/2 (Na_2SO_4)	a=1	a=2	a=3	a=4	a=5	a=6	a=7	a=8	a=9	a=10
Fe^{2+}=b b $FeSO_4$	$Na_xFe_Y(SO_4)_z$ (x=a: y=b: z=a/2+b) (theoretical capacity /mAh g^{-1})	A1	A2	A3	A4	A5	A6	A7	A8	A9	A10
b=1	B1	2:2:3 (120.24)	2:1:2 (91.19)	6:2:5 (73.44)	4:1:3 (61.48)	10:2:7 (52.87)	6:1:4 (26.33)	14:2:9 (34.53)	8:1:5 (37.23)	18:2:11 (50.76)	10:1:6 (31.09)
b=2	B2	2:4:5 (71.51)	2:2:3	6:4:7 (103.72)	2:1:2	10:4:9 (96.51)	6:2:5	14:4:11 (66.93)	4:1:3	18:4:13 (56.85)	10:2:7
b=3	B3	2:6:7 (50.89)	2:3:4 (89.68)	2:2:3	4:3:5 (108.90)	10:6:11 (99.18)	2:1:2	14:6:13 (84.39)	8:3:7 (78.54)	6:2:5	10:3:8 (68.97)
b=4	B4	2:8:9 (39.50)	2:4:5	6:8:11 (97.98)	2:2:3	10:8:13 (111.37)	6:4:7	14:8:15 (97.05)	2:1:2	18:8:17 (85.89)	10:4:9
b=5	B5	2:10:11 (32.27)	2:5:6 (59.46)	6:10:13 (82.68)	4:5:7 (102.74)	2:2:3	6:5:8 (113.04)	14:10:17 (106.65)	8:5:9 (100.94)	18:10:19 (95.82)	2:1:2
b=6	B6	2:12:13 (27.28)	2:6:7	2:4:5	2:3:4	10:12:17 (105.82)	2:2:3	14:12:19 (114.18)	4:3:5	6:4:7	10:6:11
b=7	B7	2:14:15 (23.63)	2:7:8 (44.47)	6:14:17 (63.00)	4:7:9 (79.57)	10:14:19 (94.48)	6:7:10 (107.97)	2:2:3	8:7:11 (115.00)	18:14:23 (110.21)	10:7:12 (105.79)
b=8	B8	2:16:17 (20.84)	2:8:9	6:16:19 (56.29)	2:4:5	10:16:21 (85.33)	6:8:11	14:16:23 (109.56)	2:2:3	18:16:25 (115.62)	10:8:13
b=9	B9	2:18:19 (18.63)	2:9:10 (35.52)	2:6:7	4:9:11 (64.93)	10:18:23 (77.81)	2:3:4	14:18:25 (100.64)	8:9:13 (110.8)	2:2:3	10:9:14 (116.13)
b=10	B10	2:20:21 (16.75)	2:10:11	6:20:23 (23.21)	2:5:6	2:4:5	6:10:13	14:20:27 (46.53)	4:5:7	18:20:29 (58.50)	2:2:3

*A1=$Na_xFe_Y(SO_4)_z$ (x=1 : y=b : z=1/2+b); A2=$Na_xFe_Y(SO_4)_z$ (x=2 : y=b : z=1+b); A3=$Na_xFe_Y(SO_4)_z$ (x=3 : y=b : z=3/2+b); A4=$Na_xFe_Y(SO_4)_z$ (x=4 : y=b : z=2+b); A5=$Na_xFe_Y(SO_4)_z$ (x=5 : y=b : z=5/2+b); A6=$Na_xFe_Y(SO_4)_z$ (x=6 : y=b : z=3+b); A7=$Na_xFe_Y(SO_4)_z$ (x=7 : y=b : z=7/2+b); A8=$Na_xFe_Y(SO_4)_z$ (x=8 : y=b : z=4+b); A9=$Na_xFe_Y(SO_4)_z$ (x=9 : y=b : z=9/2+b); A10=$Na_xFe_Y(SO_4)_z$ (x=10 : y=b : z=5+b); ……; An=$Na_xFe_Y(SO_4)_z$ (x=n : y=b : z=n/2+b);

B1=$Na_xFe_Y(SO_4)z$ (x=a : y=1: z=a/2+1); B2=$Na_xFe_Y(SO_4)_z$ (x=a : y=2 : z=a/2+2); B3=$Na_xFe_Y(SO_4)_z$ (x=a : y=3 : z=a/2+3); B4=$Na_xFe_Y(SO_4)_z$ (x=a : y=4 : z=a/2+4); B5=$Na_xFe_Y(SO_4)_z$ (x=a : y=5 : z=a/2+5); B6=$Na_xFe_Y(SO_4)_z$ (x=a : y=6 : z=a/2+6); B7=$Na_xFe_Y(SO_4)_z$ (x=a : y=7 : z=a/2+7); B8=$Na_xFe_Y(SO_4)_z$ (x=a : y=8 : z=a/2+8); B9=$Na_xFe_Y(SO_4)_z$ (x=a : y=9 : z=a/2+9); B10=$Na_xFe_Y(SO_4)_z$ (x=a : y=10 : z=a/2+10); ……; Bn=$Na_xFe_Y(SO_4)_z$ (x=a : y=n : z=a/2+n);

Table S2. Detailed structural information and refinement results of bare NFS material, according to the XRD pattern and associated Rietveld refinement analysis as shown in Figure S1c.

NFS ($Na_6Fe_5(SO_4)_8$). Monoclinic, space group *C2/c*,
a=11.8283608 Å, b=12.2862269 Å, c=6.5017825 Å, β=95.46234°, and V=940.58685 Å
weighted profile R factor, R_{wp}: 7.30 %, square of reflection-based R factor, R_{F2}: 10.53 %

Atom	x	y	z	frac	mult	Uiso
Na1	0.41239	0.66228	0.78681	1.00000	4	0.00631
Na2	0.00000	0.00000	0.00000	0.50000	4	0.01604
Na3	0.59358	0.84003	0.24533	0.50000	4	0.03451
Fe1	0.73232	0.14284	0.21902	1.00000	8	0.00511
S1	0.00000	0.81718	0.61372	1.00000	4	0.00372
S2	0.75216	0.57430	0.86101	1.00000	8	0.00392
O1	0.75726	0.69444	0.60565	1.00000	8	0.00810
O2	0.09274	0.86921	0.52864	1.00000	8	0.00749
O3	0.47995	0.17190	0.42090	1.00000	8	0.00932
O4	0.39223	0.98578	0.11264	1.00000	8	0.00863
O5	0.39561	0.48589	0.73085	1.00000	8	0.00942
O6	0.33882	0.23124	0.01919	1.00000	8	0.00657

Table S3. Detailed structural information and refinement results of NFS@5%CNTs composite material, according to the XRD pattern and associated Rietveld refinement analysis as shown in Figure 1b.

NFS@5%CNTs ($Na_6Fe_5(SO_4)_8$@5%CNTs). Monoclinic, space group *C2/c*,
a=11.8314687 Å, b=12.2745127 Å, c=6.4974689 Å, β=97.38121°, and V=938.892742 Å
weighted profile R factor, R_{wp}: 5.06 %, square of reflection-based R factor, R_{F2}: 9.26 %

Atom	x	y	z	frac	mult	Uiso
Na1	0.41239	0.66218	0.78491	1.00000	4	0.00731
Na2	0.00000	0.00000	0.00000	0.50000	4	0.01554
Na3	0.59358	0.84003	0.24435	0.50000	4	0.04451
Fe1	0.73527	0.16159	0.22112	1.00000	8	0.00392
S1	0.00000	0.79843	0.61257	1.00000	4	0.00308
S2	0.76723	0.57438	0.86101	1.00000	8	0.00376
O1	0.768492	0.69444	0.60565	1.00000	8	0.00785
O2	0.09274	0.86921	0.53584	1.00000	8	0.00775
O3	0.46799	0.17190	0.42095	1.00000	8	0.00926
O4	0.39547	0.99687	0.10829	1.00000	8	0.00768
O5	0.39461	0.48589	0.73258	1.00000	8	0.00624
O6	0.33824	0.23047	0.01907	1.00000	8	0.00765

Table S4. Voltage differences between anodic and cathodic CV peaks of different redox couples recorded in the first and fifth CV cycles of bare NFS and NFS@5%CNTs cathode materials as shown in Figure S7.

Sample	First cycle			Fifth cycle		
	anodic	cathodic	△E/eV	anodic	cathodic	△E/eV
NFS	3.73	3.38	0.35	3.53	3.33	0.20
	4.16	3.68	0.48	3.88	3.68	0.20
NFS@5%CNTs	3.74	3.34	0.40	3.51	3.29	0.21
	4.16	3.83	0.33	3.85	3.72	0.13
				4.10	3.92	0.18

Table S5. Slopes of fitting lines revealing the relationship between anodic and cathodic peak currents (i_p) and the square root of scan rates ($v^{1/2}$) of bare NFS, NFS@5%CNTs, and NFS@10%CNTs cathode materials as shown in Figure S8.

Sample	Slopes					
	Peak 1	Peak 2	Peak 3	Peak 4	Peak 5	Peak 6
NFS	0.2625	0.2362		-0.2586	-0.2685	
NFS@5%CNTs	0.4366	0.3696	0.2404	-0.3085	-0.3995	0.3376
NFS@10%CNTs	0.4622	0.4377	0.3365	-0.3497	-0.5239	-0.3820

Table S6. Sodium ion diffusion coefficients (D_{Na+}) of bare NFS, NFS@5%CNTs, and NFS@10%CNTs cathode materials, according to CV measurements as shown in Figure S8.

Sample	Diffusion coefficients of Na^+, D_{Na+}×10^{-13}/cm^2 s^{-1}					
	Peak 1	Peak 2	Peak 3	Peak 4	Peak 5	Peak 6
NFS	1.526	1.236		1.482	1.268	
NFS@5%CNTs	4.225	3.028	1.281	2.118	3.538	2.526
NFS@10%CNTs	4.735	4.237	2.511	2.711	6.084	3.234

Table S7. Comparison of electrochemical performance among the full NFS@5%CNTs//HC cell in this work and reported full sodium-ion batteries in the literatures.

Full Cell Configuration	Voltage / V	Rate / mA g^{-1}	Specific Capacity * / mAh g^{-1}	Energy Density / Wh kg^{-1}
This work	3.6	12	95	342
C-$NaCrO_2$ //SnO_2/rGO[1]	3	52.5	110	330
NaxFe[Fe$(CN)_6$] //FeO_x CNT[2]	2	250	60	136
$Na_3V_2(PO4)_3C$ //Sb@TiO_{2-x}[3]	2.5	660anode	250	151/61
$Na_3V_2(PO_4)_3$rGOCNT //$Na_3V_2(PO_4)_3$rGOCNT[4]	1.7	1100	90	150
P2-$Na_{2/3}Ni_{1/3}Mn_{2/3}O_2$ //Sb[5]	2.9	500	334	110
$Na_{0.8}Ni_{0.4}Ti_{0.6}O_2$ //$Na_{0.8}Ni_{0.4}Ti_{0.6}O_2$[6]	2.8	20	85	96

*Specific capacities of all the full sodium-ion batteries were calculated based on the weight of active cathode materials.

References

1 C.-H. Jo, J.-H. Jo and S.-T. Myung, *J. Alloy. Compd.*, 2018, **731**, 339-346.

2 H. Ye, Y. Wang, F. Zhao, W. Huang, N. Han, J. Zhou, M. Zeng and Y. Li, *J. Mater. Chem. A*, 2016, **4**, 1754-1761.

3 N. Wang, Z. Bai, Y. Qian and J. Yang, *Adv. Mater.*, 2016, **28**, 4126-4133.

4 C. Zhu, P. Kopold and P. A. Aken, J. Maier, Y. Yu, *Adv. Mater.*, 2016, **28**, 2409-2416.

5 L. Liang, Y. Xu, C. Wang, L. Wen, Y. Fang, Y. Mi, M. Zhou, H. Zhao and Y. Lei, *Energy Environ. Sci.*, 2015, **8**, 2954-2962.

6 S. Guo, H. Yu, P. Liu, Y. Ren, T. Zhang, M. Chen, M. Ishida and H. Zhou, *Energy Environ. Sci.*, *2015,* **8**, 1237-1244.